JOURNAL OF OPTOELECTRONICS AND ADVANCED MATERIALS, Vol. 10, No. 12, December 2008, p. 3336 - 3340

Site selectivity of iron doped in silica-bismuthate heavy metal glass systems

M. TODEA*, S. SIMON , V. SIMON
Babes-Bolyai University, Faculty of Physics & Institute for Interdisciplinary Experimental Research, Cluj-Napoca, Romania

Heavy metal glasses have attracted large interest due to their physical properties, such as high polarisability, long infrared cut-off or high non-linear optical susceptibility, optical transmission devices, ultrafast optical switches [1]. These properties can be influenced by doping with transition metal oxide.Fe^{3+} electron paramagnetic resonance (EPR) studies on iron doped silica-bismuthate glasses and glass ceramics were carried out in order to evidence the site selectivity of iron in the local structure of samples as the ratio between Bi_2O_3 and SiO_2 content changes from 9/1 to 2/3. The environment of the resonant Fe^{3+} ions was investigated in vitreous and partially crystallised samples of similar composition. EPR data indicate that the iron dopant occupy equivalent sites in glasses, in the entire composition range, while in vitroceramic samples the iron is differently disposed in samples as Bi_2O_3/SiO_2 ratio decreases. Structural changes induced by temperature rising in binary silico-bismuthate glasses are investigated by differential thermal analysis (DTA).

(Received November 1, 2008; accepted November 27, 2008)

Keywords: Heavy metal glasses, Glass-ceramic, EPR, DTA

1. Introduction

Bismuth oxide, Bi_2O_3 , is not a classical glass network former, due to its high polarizability but in the presence of conventional glass formers, it may build a glass network of [BiO_3] pyramids [1, 2]. In all optical switching and broadband amplification devices are used glasses based on bismuth oxide [3] characterised by high non-linear optical susceptibility. Bismuth-silicate glasses acquired special applications as low loss optical fibres, infrared transmitting materials or as active medium of Raman-active fibre optical amplifiers and oscillators [4-7]. Bismuth based glasses are also used to produce after appropriate annealing high temperature superconductors with controllable microstructure [8-10].

The structural role played by Bi_2O_3 in glasses without or with low content of conventional glass formers, so called heavy metal glasses, is complicated and poorly understood. The problem is complex because the [BiO_n] polyhedra are highly distorted due to lone pair electrons and consequently the structural model for $xSiO_2 \cdot (100\text{-}x)Bi_2O_3$ glasses is under discussion [11, 12].

Several techniques have been employed in the attempt to identify the local environment of the different elements in bismuthate glasses. Electron paramagnetic resonance (EPR) spectroscopy is a very useful experimental technique in obtaining information on the local structure around transition metal ions in glasses [13-15]. The transition metal ions can be used to probe the host glass structure, because their outer d-electron orbital functions have rather broad radial distributions and their responses to surroundings cations are very sensitive. Due to the lack of structural long range order in amorphous materials a unambiguous assignment of the structural groups is not possible without comparing their spectra with those of corresponding crystalline counterparts.

This paper is focused on the structural changes induced in iron doped silica-bismuthate glasses by progressive replacing of Bi_2O_3 with SiO_2, by crystallisation heat treatment and by temperature rising.

2. Experimental

Glass samples belonging to $0.01Fe_2O_3 \cdot 0.99[xSiO_2 \cdot (100\text{-}x)Bi_2O_3]$ system ($10 \leq x \leq 60$ mol %) were prepared using $BiO(NO_3) \cdot H_2O$, SiO_2 and Fe_2O_3 of analytical grade purity. Corresponding amounts of reagents were mixed and melted in sintercorundum crucibles for 10 minutes at 1200°C. The samples were obtained by fast quenching of the melts cast and pressed between steel plates at room temperature. X-ray powder diffraction analysis did not reveal any crystalline phase. The vitreous samples were partially crystallised by heat treatment applied at 600°C for 24 hours.

Thermal analysis measurements were carried out using a MOM derivatograph. Thermogravimetric, differential thermogravimetric and differential thermal analysis curves were recorded from powder samples, with a rate of 10°C/min, up to 1000°C in static air atmosphere, using Al_2O_3 as reference material.

Electron paramagnetic resonance spectra were recorded on powder samples at room temperature in X band, with 4 G modulation amplitude, on an ADANI spectrometer.

3. Results

The phase diagram given in Fig. 1 shows that Bi_2O_3 and SiO_2 can form a binary system by melting of oxide mixtures in air atmosphere.

DTA is primarily used for detection of transitions induced by temperature rising. The thermogravimetric (TG) and differential thermogravimetric (DTG) curves evidence in the run temperature range no mass loss for the investigated glasses. In the differential thermal analysis (DTA) curves (Fig. 3) are evidenced both exothermic and endothermic events summarised in Table 1.

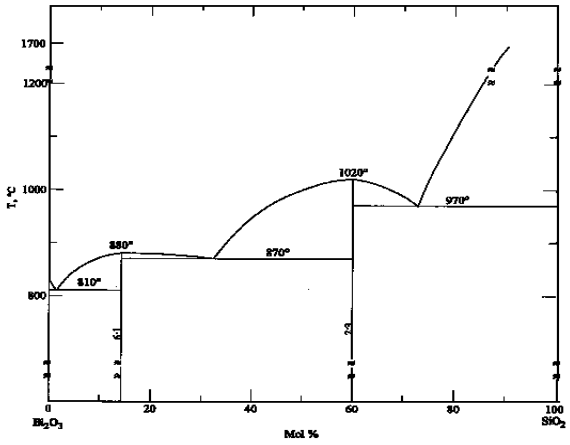

Fig. 1. Phase diagram of binary Bi_2O_3- SiO_2 system according to Ref. [16].

The silica-bismuthate samples doped with 1 mol % Fe_2O_3 are transparent and coloured from yellow-brown to red-brown as SiO_2 content increases from 10 to 60 mol %.

The X-ray diffraction patterns show a very large peak typical for glass systems and prove their vitreous state. The crystalline phases identified from X-ray diffractograms of heat treated samples (Fig. 3) are $Bi_{12}SiO_{20}$, a δ solid solution $Bi_{5.6}Si_{0.5}O_{9.4}$ and Bi_2SiO_5 [17]. The $Bi_{12}SiO_{20}$ phase is present in samples with $10 \leq x \leq 30$, $Bi_{5.6}Si_{0.5}O_{9.4}$ phase in samples with $40 \leq x \leq 60$ and Bi_2SiO_5 phase is observed, in a low amount for the sample with x=60.

The room temperature EPR spectra of all glass samples are shown in Fig. 4. The spectra consist of a main relative large resonance line with $g_{eff} \approx 4.3$ and a very weakly resolved line at $g_{eff} \approx 2.0$. The EPR line at $g \approx 4.3$ is occurring in all glasses containing Fe^{3+} ions as impurity or as dopant [18-21]. The dependence of the width of this line with glass samples composition is illustrated in Fig. 5a. The feature of Fe^{3+} EPR spectra for heat treated samples are evidently modified, as can be seen in Fig. 6. For low SiO_2 contents ($x \leq .30$) the dominant line occurs at $g_{eff} \approx 2.0$ along with the less intense line at $g_{eff} \approx 4.3$, while for higher SiO_2 contents ($40 \leq x \leq 60$) the $g_{eff} \approx 2.0$ signal is slightly evidenced, excepting the sample with x = 60. The width of $g_{eff} \approx 2.0$ line, recorded from samples with low SiO_2 content, decreases with x as can be observed from Fig. 5b.

4. Discussion

The differential thermal analysis (DTA) curves show a very broad endothermic peak corresponding to the glass transition. This transition is followed by more than one exothermic peak which show different stages of crystallisation denoting that the silico-bismuthate glasses are not characterised by a unique crystallisation mechanism.

Several exothermic peaks could be also related to the fact that crystalline Bi_2O_3 can form several polymorphs [11].

We consider more probable that the less intense exothermic peaks recorded before the most intense one could be associated with the structural relaxation and germs nucleation in the solid glass network, the most intense exothermic peak with the cold partial crystallisation process and the next ones with structural polymorph modifications of the prevalent crystalline phase.

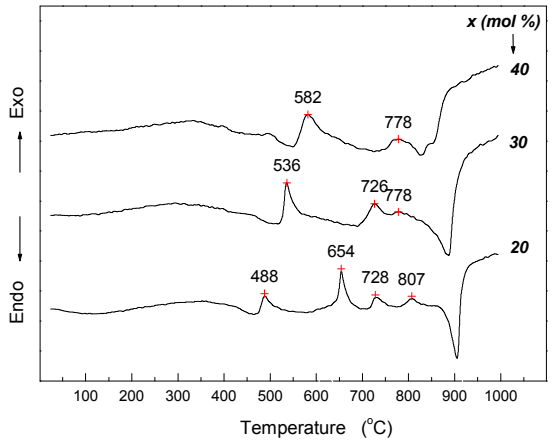

Fig. 2. DTA curves of $xSiO_2 \cdot (100\text{-}x)Bi_2O_3$ glasses.

According to another approach [22] the exothermic DTA peaks recorded from iron phosphate glasses are due to the crystallisation of structural units including different oxidation states of the modifier cations. The shift of the crystallisation peak toward lower temperature is determined by increasing number and size of nucleation centres [23]. This could be an explanation for the composition dependence of the crystallisation temperature (Table 1) showing that by increasing of the bismuth content are increasing also the number of nucleation centres.

Table 1. Temperature of exothermic (T_{exo}) and endothermic (T_{endo}) peaks, glass transition temperature (T_g) und Hruby parameter (K_{gl}) for $xSiO_2 \cdot (100\text{-}x)Bi_2O_3$ glasses.

X (mol %)	T_{exo} (°C)	T_{endo} (°C)	T_g (°C)	K_{gl}
20	488, 654, 728, 807	905	415	0.19
30	536, 726, 778	887	412	0.35
40	582, 778	826	400	0.53

At the same time the glass stability expressed by Hruby parameter [24] evidence the same composition dependence (Table 1). The Hruby parameter $K_{gl} = (T_{cr}-T_g)/(T_m-T_{cr})$ was calculated considering for T_{cr} the temperature of the first exothermic peak, T_g the glass transition temperature and T_m the melting temperature.

The crystalline phases $Bi_{12}SiO_{20}$ and $Bi_{5.6}Si_{0.5}O_{9.4}$ identified in X-ray diffractograms of heat treated samples with $x \leq 60$ (Fig. 3) evidence different configurations of the component atoms in phases of almost the same Bi/Si ratio and same oxygens number ($Bi_{12}SiO_{20}$ vs. $Bi_{11.2}SiO_{18.8}$).

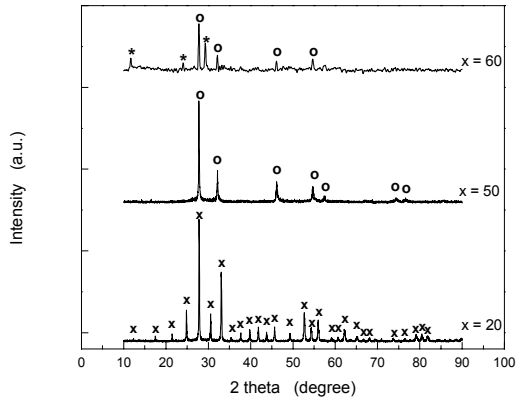

*Fig 3. X-ray diffraction pattern of glass ceramics samples (**x**-$Bi_{12}SiO_{20}$, **o**-$Bi_{5.6}Si_{0.5}O_{9.4}$, and ***-Bi_2SiO_5).*

The expected crystalline phases with higher silicon content, like Bi_2SiO_5 [14, 25], are observed, in a low amount, only for the sample with x=60. The development of 12:1 and δ type crystalline phases in glass samples with $x \leq 50$ shows that in these glasses, which appear macroscopic completely homogeneous, there are small regions rich in silicon, quite stable and regions rich in bismuth, that will easily crystallise in δ phase[26]. It was suggested [12] that the structure of glasses with x = 50 mol % is similar with that of Bi_2SiO_5 crystal, that is a structure formed from continuous [SiO_n] chains placed between double layers of [BiO_n] units. The growth of a δ crystalline phase in our sample with x = 50 instead of the expected Bi_2SiO_5 phase support the above invoked phase separation rather than a layered structure.

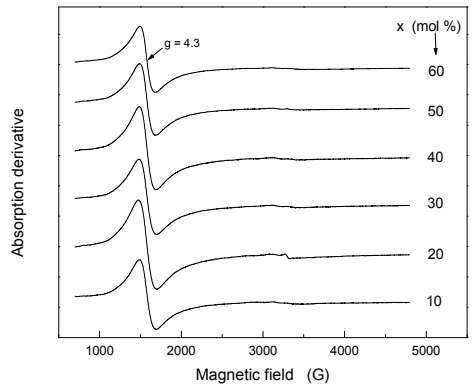

Fig. 4Fe^{3+} EPR spectra of glass samples $0.01Fe_2O_3 \cdot 0.99[xSiO_2 \cdot (100-x)Bi_2O_3]$.

The features of the EPR spectra for different Bi_2O_3/SiO_2 ratio are quite similar for all glass samples (Fig. 4) and consist in lines at g = 2.0 and g = 4.3. The lines at g = 2.0 are assigned to paramagnetic ions in sites characterized by relatively weak crystalline fields, for which Zeeman term dominates, while the lines with g > 2 are attributed to paramagnetic ions in sites of relatively strong crystal field, where the crystal field terms are comparable or larger than the Zeeman term [27]. However one can observe that the width of g_{eff} = 4.3 resonance line broadens when SiO_2 content increases from 10 to 20 mol % and by further replacing of Bi_2O_3 with SiO_2 the linewidth narrows (Fig.5a).

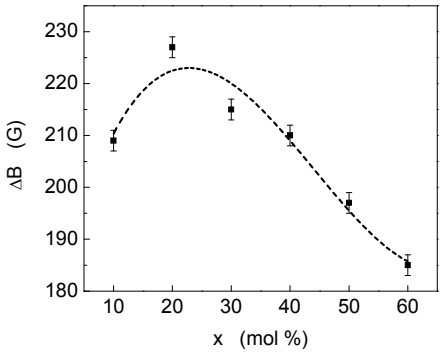

a)

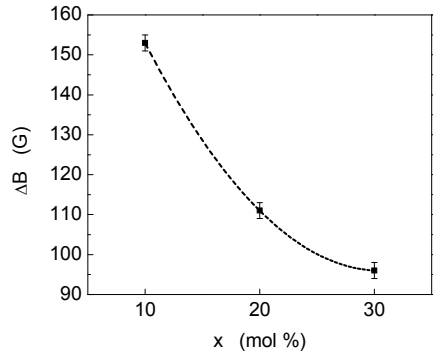

b)

Fig. 5 a) Composition dependence of the width of resonance line with g = 4.3 recorded from glass samples. b) Composition dependence of the width of resonance line with g = 2.0 recorded from vitroceramic samples.

In order to account for this evolution of the width of Fe^{3+} resonance line we consider that the initial broadening is correlated with the increase of disorder on the sites of iron from the glass sample with x = 20 compared to the sample with x = 10.

The narrowing of the resonance line for x > 20 denotes a more uniform environment of Fe^{3+} ions in silica rich glasses. The shape of the EPR line describes both the disorder around the resonant iron ions and the structural characteristic of the glass matrices in which these ions are incorporated. From the last point of view the EPR spectra of the investigated samples show that in the much polymerised

silica network the disorder degree quenched from the melt is lower than in the more fragmented network from the matrices with high bismuth content.

In the heat treated samples the iron ions are subjected to modified crystal fields and the Fe^{3+} EPR spectra (Fig. 6) show the changes occurred in the local order around the iron ions. Taking into account the ionic radii for Bi^{3+} and Fe^{3+} ions and their identical valence state, it is expected that Fe^{3+} ions are occupying Bi^{3+} sites from $Bi_{12}SiO_{20}$ crystalline phase.

One also remarks that the width of this line narrows with increasing SiO_2 content (Fig.5b) that denotes the tendency to more structural order around the resonant Fe^{3+} ions disposed on these sites.

The signal at $g_{eff} = 4.3$ is recorded from all samples and the linewidth is close to 200 G for all compositions. This result indicates that the short-range order surrounding the Fe^{3+} ions responsible for this signal is still characterized by a relatively strong crystalline field and can be associated with iron sites in silica-rich non-crystalline network. The line with g = 2.0 is clearly resolved only for lower SiO_2 contents, up to x = 30, and is assigned to Fe^{3+} ions situated in sites of low crystal field with octahedral symmetry.
The weakly developed resonance line assigned to iron ions disposed in sites of low crystal field for vitroceramic samples with x > 30 mol % show that only a small amount of Fe^{3+} ions are situated in the Bi^{3+} sites of δ phase, their surrounding being highly distorted.

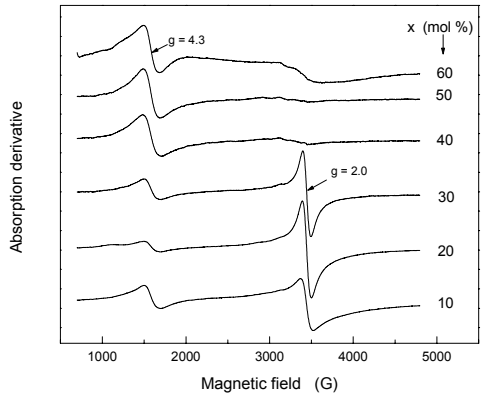

Fig. 6 Fe^{3+} EPR spectra of vitroceramic samples $0.01Fe_2O_3 \cdot 0.99[xSiO_2 \cdot (100-x)Bi_2O_3]$.

The blocking effect of the lone pair electrons of Bi^{3+} ions [11, 12, 28, 29] may also contribute to this result. It is possible that the majority of Fe^{3+} ions are disposed in the remained non-crystalline silica-rich phase.

5. Conclusions

The EPR results show that the iron environment in silica-bismuthate glass matrices is characterised by a higher ordering when SiO_2 replace more than 20 mol % of Bi_2O_3. The highest disorder degree around iron in glass samples is noticed for x = 20. For all compositions in glass samples the iron ions occupy sites of strong crystal field, while in the partially crystallised samples, up to x = 30, iron ions are identified both in sites of strong crystal field and in sites of low crystal field. The EPR data also indicate that the fragmentation of the glass network is much pronounced in the high bismuth content range.

The development of only δ type solid solution crystalline phase in the heat treated samples with high SiO_2 content, $x \geq 40$, even though their composition is much closer to Bi_2SiO_5 phase, proves that in the corresponding precursor glasses there are small regions with high bismuth content that will easily crystallise in a δ phase and regions rich in silica, more stable as non-crystalline phase.

References

[1] W. H. Dumbaugh, Phys. Chem. Glasses, **27** 119 (1986).
[2] D. Sreenivasu, V. Chandramouli, Bull. Mater. Sci. **23**(4), 281(2000).
[3] N. Sugimoto, Am. Ceram. Soc. **85**(5), 1083 (2002).
[4] J. Yang, S. Dai, N. Dai, S. Xu, L. Wen, L. Hu, Z. Jiang, J. Opt. Soc. Am. B **20**(5), 810 (2003).
[5] W.H. Dumbaugh, J.C. Lapp, J. Am. Ceram. Soc. **75**(9), 2315 (1992).
[6] E.M. Vogel, Phys. Chem. Glasses, **32** 231 (1991).
[7] Z. Pan, D.O. Henderson, S. H. Morgan, J. Non-Cryst. Solids, **171,** 134 (1994).
[8] T. Komatsu, R. Sato, K. Imai, K. Matusita, T. Yamashita, Jap. J. Appl. Phys. **27,** L550 (1998).
[9] D. G. Hinks, L. Soderholm, D. W. Capone II, B. Dabrowski, A. W. Mitchell, D. Shi, Appl. Phys. Lett. **53,** 423 (1988).
[10] T. Minami, Y. Akamatsu, M. Tatsumisago, N. Toghe, Y. Kowada, Jap. J. Appl. Phys., **27,** L777 (1998).
[11] A. Witkowska, J. Rybicki, A. DiCicco, 6-thInternational Conference on Intermolecular Interactions in Matter, Gdańsk – Poland, 10-13 September (2001).
[12] T. Nanba, H. Tabuchi, Y. Miura, Proceedings of XX Int. Congress. Glass, Sept. 27- Oct. 1, Tokyo, Japan, P-10-011 (2004).
[13] A. Abragam, B. Bleaney, Electron Paramagnetic Resonance of Transition Ions, Clarendon Press, Oxford, (1970).
[14] D. L. Griscom, J. Non-Cryst. Solids, **40**, 211(1980).
[15] J. Wong, C.A. Angell, Glass structure by spectroscopy, Marcell Dekker Inc., New York, 197610 .
[16] V. M. Skorikov, P. F. Rza-Zade, Yu. F. Kargin, F. F. Dzhalaladdinov, Zh. Neorg. Khim **26**(4), 1070 (1981).
[17] G. Gattow, H. Schroeder, Z. Anorg. Allg. Chem., **318**, 176 (1962).
[18] R.H. Sands, Phys. Rev., **99**, 1222 (1955).
[19] R. Stößer, M. Notz, Glastechn. Ber. Glass Sci. Technol., **67** 156 (1994).
[20] S. Simon, R. Pop, V. Simon, M. Coldea, J. Non-Cryst. Solids, **331**, 1 (2003).

[21] R. Berger, J. Kliava, E.M. Yahiaoui, J.-C. Bissey, P. K. Zinsou, P. Beziade, J. Non-Cryst. Solids **180**, 151 (1995).
[22] X. Fang, C. S. Ray, A. G. Milankovoc, D. E. Day, J. Non-Cryst. Solids, **283**, 162 (2001).
[23] T. Wakasugi, T. Kadoguchi, R. Ota, J. Non-Cryst. Solids, **290**, 64 (2001).
[24] S. Simon, V. Simon, Mat. Lett, **58,** 3778 (2004).
[25] Y. T. Fei, S.J. Fan, R.Y. Sun, J.Y. Xu, J. Mat. Sci. Lett, **19,** 893 (2000).
[26] M. Todea, S. Simon, J. Optoelectron. Aadv. Mater. **9**, (3), 621 (2007).
[27] T. Castner, C.S. Newell, W.C. Holton, C.P. Schlichter, J. Chem. Phys., **32,** 668 (1960).
[28] Y. Wu, M. J. Forbess, S. Seraji, S.J. Limmer, T. P. Chou, C. Nguyen, G. Cao, J. Appl. Phys **90(**10), 5296 (2001).
[29] A. Pan, A. Ghosh, J. Chem. Phys. **112(**3), 150 (2000).

*Corresponding author: todeam@phys.ubbcluj.ro